

Original Research Article

Use of satellite-based leaf area index data for monitoring green gram crop growth in Ikombe-Katangi area, Machakos county, Kenya

Abstract

Monitoring the conditions under which crops grow and estimating their yield is essential to the process of economic development in any nation. The traditional approaches to crop monitoring are labor- and resource-intensive, as well as limited in their ability to cover expansive geographic regions. Since remote sensing data is integrated with ground measurements, it has been used as a potentially useful tool to extract biophysical variables such as leaf area index (LAI), biomass, and phenology. Leaf Area Index (LAI) is a key variable that bridges remote sensing observations to the quantification of agroecosystem processes such as yield. Confirming the potential role that satellite-based LAI could play in crop health monitoring was the purpose of this study. High resolution leaf area index was retrieved from Landsat 8 OLI imageries, and ground leaf area index measurements were taken in Ikombe-Katangi Machakos in Machakos county. An equation based on regression was developed to estimate the leaf area index using the normalized difference vegetation index that was derived from Landsat-8 OLI (NDVI). According to the findings, the derived LAI exhibited strong linear relationships with the leaf area index that was measured on the ground for green gram crops, with RMSE values being 0.09846, and R² values of 0.9249. The overall findings shed light on the viability of using multispectral data, in estimating leaf area index in a very fragmented agricultural landscape, such as that found in the Ikombe and Katangi areas of Machakos, Kenya. Therefore, accurate crop monitoring on a large scale can be accomplished through remote sensing data in conjunction with LAI measurements taken from the ground. The implementation of the leaf area index is subject to the environmental condition which requires to be investigated as the use of remote sensing data is advocated for.

Key words; Leaf Area Index, Satellite data, Normalized Vegetation Index, Enhanced Vegetation Index, Landsat 8, Remote Sensing

INTRODUCTION

The leaf area index, or LAI, is a measurement that can be used to quantify the amount of live green leaf material that is present in the canopy of a given area (Chen & Black, 1992). It is utilised in the estimation of photosynthesis, evapotranspiration, crop yield, and other physiological processes in the field of agroecosystem research (Demarty et al., 2007).

The Leaf Area Index, which is also known as LAI, is a measurement that does not have any dimensions and is based on the ratio of the leaf area on one side (measured in m²) to the ground surface area (measured in m²) (Asner et al., 2003). It has been known for a very long time that the leaf area index (LAI) is a good indicator for a variety of different agronomic, ecological, and hydrological applications. Some examples of these applications include modelling atmospheric circulation (Reyes-González et al., 2019), photosynthesis and biomass accumulation (Fassnacht et al., 1997), and evapotranspiration (Fassnacht et al., 1997). Other applications include analyzing the condition of the surrounding vegetation (Reyes) (Jung et al. 2010).

Remote sensing has proved to be a promising alternative tool for estimating crop LAI quickly over large areas, and without damaging the canopy (Qi et al., 2000, Mourad et al., 2020). The retrieval of crop biophysical variables from remote sensing falls into two categories: empirical and physical modeling approaches. The simplest method of estimating LAI from remote sensing is by establishing an empirical relationship between the remotely sensed vegetation indices (VIs) and measured LAI, referred to as the LAI-VI approach (Baret and Guyot, 1991, Broge et al., 2001). LAI has historically been measured by using in situ accurate LAI measurements but with the advent of remote sensing technologies, both in situ measurements and remotely sensed data are used hand in hand to establish the best LAI-VI relationships that can be used to estimate LAI especially over large areas (Kinane et al., 2021).

STUDY AREA

According to Fig 1.0, the wards of Katangi and Ikombe in Machakos County, Kenya are the focus of this research. The climate of the study region can be summarised as being very dry and hot on average. The Arid and Semi-Arid Lands (ASALs) are a region that can be found in the eastern part of the Sudano-Saharan belt. This region is made up of a variety of land types, such as coastal plains, upland plateaux, and isolated hill ranges, and is primarily located at an elevation of less than 1600 metres (GOK 2010). The arid regions are characterized by high average temperatures with a large range in temperature throughout the day. Rainfall in these regions is scant, sporadic, and of two modes, and it varies greatly in both location and over the course of time (Shisanya et al., 2011). The majority of rain comes in the form of

intense but brief storms, which are responsible for significant amounts of runoff and soil erosion. The arid areas typically receive between 150 and 450 millimetres of precipitation throughout the course of a year on average. The soils are extremely variable, but in general they are shallow, of light to medium texture, with low fertility, and they are susceptible to compaction, capping, and erosion (Jaetzold & Schmidt 1983). The cultivation of crops is only possible in a select few locations due to the presence of volcanic soils and alluvial deposits. Heavy clays can also be found but cultivating them is challenging due to the poor workability of the clays as well as the salinity and sodicity issues that they present. Both the availability of water and its accessibility are highly variable, which is a significant factor that inhibits production (Jaetzold & Schmidt 1983) and at the same time encourages the growing low water demanding crops such as green grams.

The study area is located within agroecological zones (AEZ) IV and V-VI, and it receives an annual rainfall totaling anywhere from 500 to 850 millimetres. They are then divided even further into four categories, based on their potential for agricultural use (Jaetzold & Schmidt 1983). These include a) semi-arid areas with mixed rain-fed and irrigation agriculture as well as high economic and political disparities; b) semi-arid areas with encroaching agro-pastoral use by marginalized smallholders; c) semi-arid areas with predominantly pastoralist use in the economic and political periphery; and d) semi-arid areas that include protected areas and their surrounding areas. Semi-arid conditions can be found in the counties of Kajiado, Narok, Mbeere, Mwingi, Kitui, Machakos, and Makueni (GOK, 2010).

Mixed crop and livestock production is the primary form of agriculture practiced in these regions. Crops are grown to satisfy the subsistence needs of the household, and any surplus is sold for monetary gain to supplement the income of the household (Gichangi et al., 2015). The lack of rainfall and the high number of pests both present significant dangers. Farmers who keep livestock, engage in mixed cropping, and plant drought-resistant crops such as cow and pigeon peas can reduce the impact of these risks on their businesses (GOK, 2002).

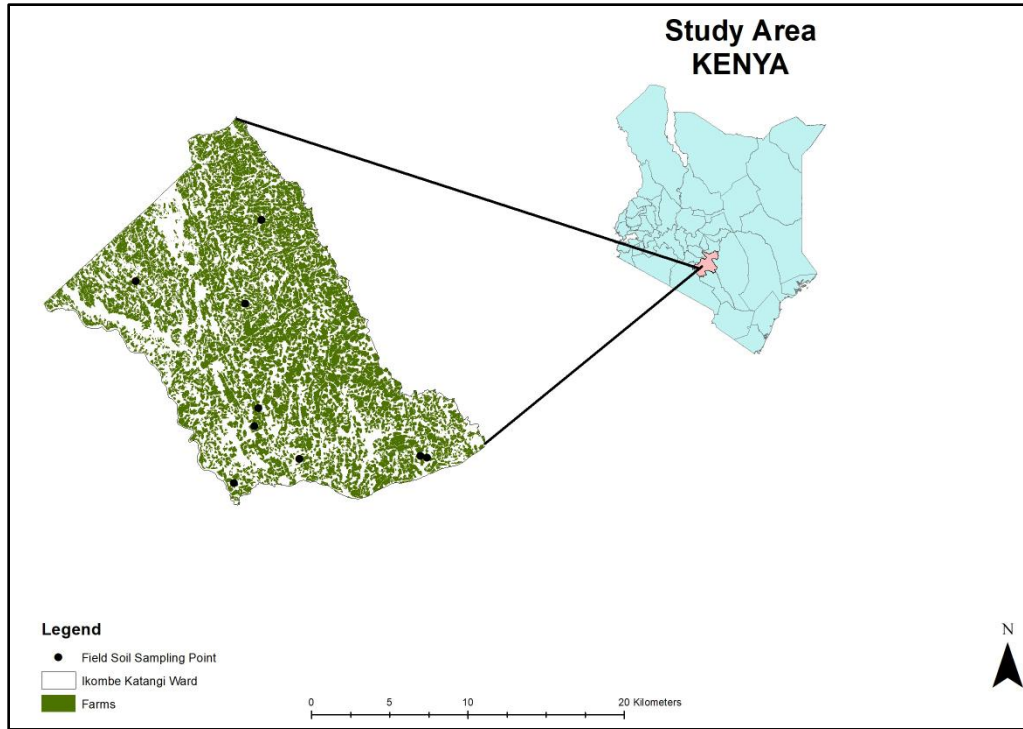


fig .1 Map showing study area in Kenya

METHOD

The vegetation index (VI) approach associated with spectral vegetation indices was used to estimate the LAI. This approach establishes a statistical relationship between remotely sensed VIs and observed LAI values, (Anav *et al.* 2013). At the beginning, normalized difference vegetation index (NDVI) and soil-related vegetation index (SR) were commonly used. Over the years, other vegetation indices have been developed; they include; Soil Adjusted Vegetation Index(SAVI), (Anav *et al.* 2013; Qi *et al.* 2000), Atmospherically Resistant Vegetation Index (ARVI) (Kaufman and Tanre. 1992), Enhanced Vegetation.

To estimate LAI, the vegetation index approach has been adopted as its easy and simple to calculate. The main challenge is the lack of In situ LAI measurement that can be used to make an LAI-VI relationship that is in accordance with the study area. Therefore, a method to calculate the LAI has been adopted from an existing LAI-VI index.

Enhanced Vegetation Index(EVI) (Matsushita *et al.*, 2007; Z. Jiang *et al.* 2008), modified triangular vegetation index (MTVI) (Long and Eitel 2008; Name and range 2004), Wide Dynamic Range Vegetation Index (WDRVI) green chlorophyll index (GCI) and Enhanced Vegetation Index 2(EVI2),(Z. Jiang *et al.*, 2008; Viña *et al.*, 2011). The equation for leaf area determination is as follows; ,

$$LAI=(2.77\sqrt{EVI2-(1.66)})^{(3/2)}.....equation 1$$

According to Kang et al., 2016, it was possible to establish that saturation is less common in relationships using EVI and EVI2 compared to NDVI, and in some cases EVI and EVI2 are linearly related to LAI, indicating an ability to resolve LAI differences over a wider range of canopy conditions. EVI2 was found to perform better than EVI in prediction power across all crops, proving that it can be used as a strong estimator of LAI when data from the blue band are not available. In this case, the global LAI-VI relationships that were built by (Kang et al. 2016), in Table 1 shows the LAI-VI relationships for specific crops as obtained from the study. It is from these relationships that equation 1 was performed that estimates the LAI of green gram crop using EVI2 vegetation index. For green gram, the coefficients for soy bean were used due to the similarity in leaf characteristics.

Table 1: Crop coefficient for various crops vegetation indices (Kang et al. 2016)

Crop Type	VI	SLR Model	Coefficient (Confidence Interval)		Prediction Model	RMSE (m ² /m ²)	MAE (m ² /m ²)	Quantiles of Absolute Residuals (m ² /m ²)				
			a	b				5%	25%	50%	75%	95%
Overall	EVI	$\sqrt{y} = ax + b$	2.07 (1.97, 2.17)	0.47	$y = (ax + b)^2$	1.13	0.89	0.06	0.33	0.70	1.38	2.24
	EVI2	$\sqrt{y} = a\sqrt{x} + b$	2.92 (2.78, 3.06)	-0.43	$y = (a\sqrt{x} + b)^2$	1.11	0.87	0.06	0.32	0.70	1.33	2.17
Row crop	EVI	$\sqrt{y} = ax + b$	2.16 (2.1, 2.32)	0.41	$y = (ax + b)^2$	1.14	0.89	0.06	0.31	0.67	1.32	2.29
	EVI2	$\sqrt{y} = a\sqrt{x} + b$	3.16 (3.01, 3.31)	-0.58	$y = (a\sqrt{x} + b)^2$	1.12	0.86	0.06	0.30	0.67	1.28	2.22
Maize	EVI	$\sqrt{y} = ax + b$	2.42 (2.21, 2.65)	0.34	$y = (ax + b)^2$	1.01	0.81	0.07	0.33	0.72	1.15	1.98
	EVI2	$y^{\frac{1}{2}} = a\sqrt{x} + b$	5.3 (4.89, 5.68)	-1.66	$y = (a\sqrt{x} + b)^{\frac{1}{2}}$	0.92	0.74	0.06	0.29	0.65	1.02	1.81
Soybean	EVI	$\sqrt{y} = ax + b$	2.53 (2.28, 2.76)	0.08	$y = (ax + b)^2$	0.69	0.49	0.02	0.14	0.32	0.68	1.45
	EVI2	$\sqrt{y} = ax + b$	2.77 (2.47, 3.03)	0.06	$y = (ax + b)^2$	0.70	0.51	0.04	0.15	0.34	0.78	1.42
Wheat	EVI	$y^{\frac{1}{2}} = ax + b$	4.24 (3.71, 4.78)	0.22	$y = (ax + b)^{\frac{1}{2}}$	1.13	0.94	0.07	0.41	0.82	1.34	2.03
	EVI2	$y^{\frac{1}{2}} = ax^{\frac{1}{2}} + b$	5.47 (4.81, 6.16)	-1.03	$y = (ax^{\frac{1}{2}} + b)^{\frac{1}{2}}$	1.13	0.94	0.12	0.41	0.87	1.37	2.12
Rice	EVI	$y^{\frac{1}{2}} = ax + b$	4.27 (3.25, 5.23)	-0.05	$y = (ax + b)^{\frac{1}{2}}$	1.03	0.79	0.07	0.35	0.67	1.02	2.38
	EVI2	$y^{\frac{1}{2}} = ax + b$	5.32 (4.08, 6.51)	-0.18	$y = (ax + b)^{\frac{1}{2}}$	1.02	0.78	0.06	0.34	0.70	1.06	2.35
Cotton	EVI	$\sqrt[3]{y} = a\frac{1}{\sqrt{x}} + b$	-1.25 (-1.39, -1.11)	2.97	$y = \left(a\frac{1}{\sqrt{x}} + b\right)^3$	0.91	0.73	0.05	0.25	0.55	1.12	1.62
	EVI2	$\sqrt[3]{y} = a\frac{1}{\sqrt{x}} + b$	-1.21 (-1.33, -1.07)	2.95	$y = \left(a\frac{1}{\sqrt{x}} + b\right)^3$	0.93	0.76	0.04	0.33	0.64	1.16	1.61
Pasture	EVI	$y^{\frac{1}{2}} = ax^2 + b$	2.84 (2.49, 3.20)	0.88	$y = (ax^2 + b)^{\frac{1}{2}}$	0.98	0.81	0.10	0.45	0.72	1.07	2.00
	EVI2	$y^{\frac{1}{2}} = ax^{\frac{3}{2}} + b$	2.99 (2.6, 3.37)	0.72	$y = (ax^{\frac{3}{2}} + b)^{\frac{1}{2}}$	0.99	0.82	0.06	0.42	0.70	1.12	1.91

Landsat 8 OLI band data was acquires from the Glovis website and converted to TOA planetary reflectance using reflectance rescaling coefficients provided in the product meta-data file (MTL file). The following equation was used to the convert the DN values to TOA reflectance for Landsat 8OLI data as follows:

$$pA' = Mp * Qcal + Ap$$

where :

pA' = TOA planetary reflectance, without correction for solar angle. Note that pA' does not contain a correction for the sun angle.

Mp = Band-specific multiplicative rescaling factor from the metadata (REFLECTANCE_MULT_BAND_x, where x is the band number).

A_p = Band-specific additive rescaling factor from the metadata (REFLECTANCE_ADD_BAND_x, where x is the band number)

Q_{cal} = Quantized and calibrated standard product pixel values (DN) TOA reflectance with a correction for the sun angle is then:

$$pA = pA' / \cos(\theta_{sz}) = pA' / \sin(\theta_{se})$$

where

pA = TOA planetary reflectance
 θ_{se} = Local sun elevation angle. The scene center sun elevation angle in degrees is provided in the meta-data (SUN_ELEVATION).

θ_{sz} = Local solar zenith angle; $\theta_{sz} = 90 - \theta_{se}$

The atmospherically corrected image was cropped to the extents of the study area.

The EVI formula was applied to the georeferenced image to obtain EVI values of the image using any GIS platform ARCGIS 10.8.

$$EVI = 2.5 * ((\text{Band 5} - \text{Band 4}) / (\text{Band 5} + 6 * \text{Band 4} - 7.5 * \text{Band 2} + 1)) \dots \dots \dots \text{Equation 2.}$$

In ARCGIS 10.8 the EVI value was calculated using the model builder tool through the calculate value tool, which allows the use of the Python math module to perform more complex mathematical operations. Once the EVI values were obtained. The EVI formulas used were;

$$EVI = G * \rho_{NIR} - \rho_{RED} / \rho_{NIR} + (C1 * \rho_{RED} - C2 * \rho_{BLUE}) + L$$

and can be rewritten as;

$$EVI = G * \rho_{NIR} / \rho_{RED} - 1 + \rho_{NIR} / \rho_{RED} + (C1 - C2 * \rho_{RED} / \rho_{RED}) + L / \rho_{RED}$$

Where:

L is a soil adjustment factor,

C1 and C2 are coefficients used to correct aerosol scattering in the red band using the blue band. The ρ_{blue} , ρ_{red} , and ρ_{nir} represent reflectance in the blue (0.45-0.52 μm), red (0.6-0.7 μm)

Near-Infrared (NIR) wavelengths (0.7-1.1 μm)

G is a gain factor.

In Landsat 8 the equation would be formulated as follows.

$$EVI=2.5*((BAND5-BAND4)/(BAND5+6*BAND4-7.5*BAND2+1))$$

where NIR corresponds to the near-infrared band (LANDSAT band 4), RED corresponds to

The red band (LANDSAT band 3), BLUE corresponds to the blue band (LANDSAT band 1)

RESULTS

Leaf Area Index parameters was extracted from remote sensing-based data for green gram under farm field conditions. The leaf area index was calculated and validated using field results from the two study areas. The LAI ranged from 1.068 to 1.77 for green gram and while field data results ranged from 1.066 to 1.833, see Figure 2.0. The observed LAI from field data and the estimated LAI from satellite data is shown in table 2. The correlation analysis was carried out between the field and satellite data and RMSE error of 0.09846 and R2 of 0.9249.

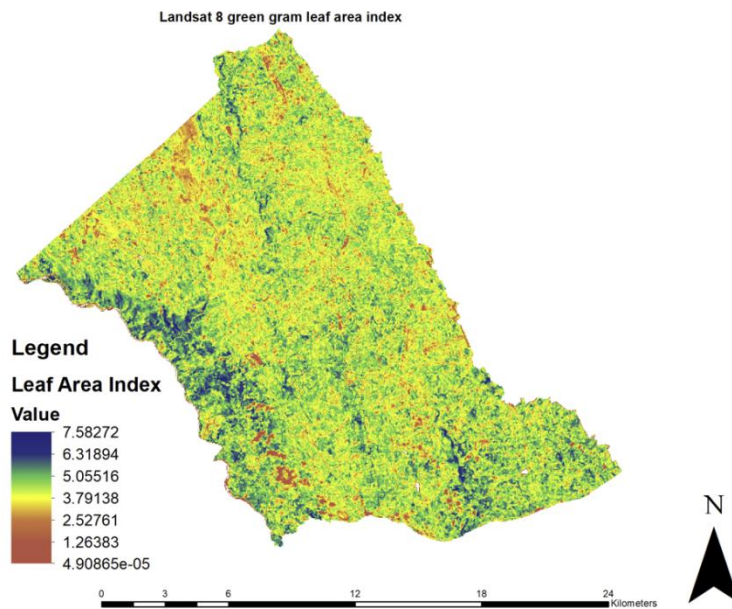


Figure 2. 0: Extracted Leaf Area Index data for Green gram crop in Ikombe-Katangi study area

Table 2: Field and remote sensing extracted Leaf Area Index Data

CROP	OBSERVED LAI	ESTIMATED LAI
GREEN GRAM	1.068	1.2333
GREEN GRAM	1.13315	1.100
GREEN GRAM	1.7425	1.8667
GREEN GRAM	1.07165	1.0667
GREEN GRAM	1.25095	1.3333

CROP	OBSERVED LAI	ESTIMATED LAI
GRAM		
GREEN	1.67	1.8333
GRAM		
GREEN	1.77275	1.7667
GRAM		
GREEN	1.7472	1.7333
GRAM		
RMSE	0.09846	

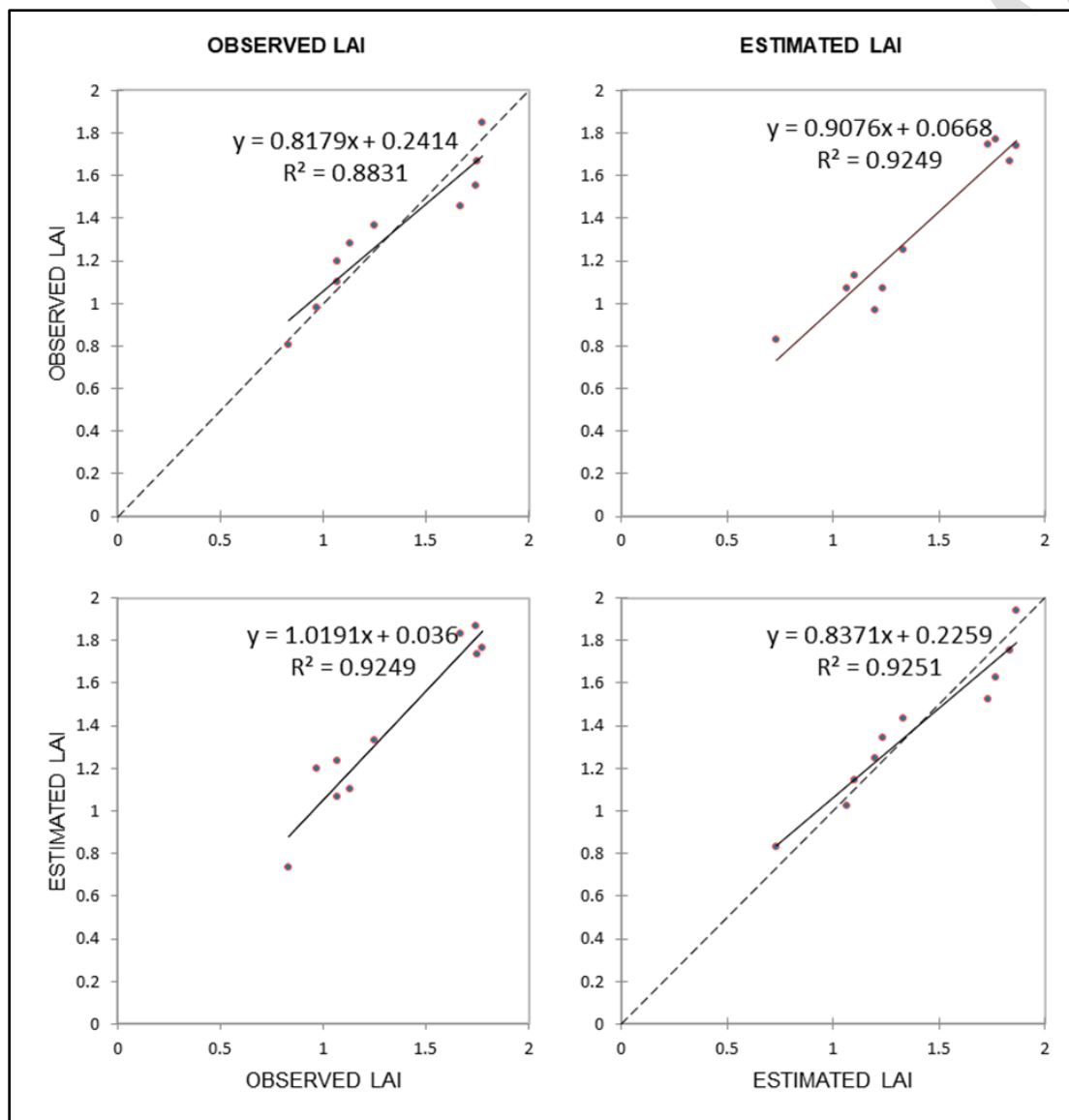


Figure 3.0: R2 results for remote sensing-based leaf area index correlations with green gram field data

DISCUSSIONS

Leaf Area Index (LAI), which is the total green leaf area (double-sided) per unit horizontal ground surface area of vegetation canopy (Watson, 1947; Fernandes et al., 2014) is an essential biophysical variable. It is used in soil-vegetation-atmosphere modeling (Laurent et al., 2014; Launay, 2005; FAO, 2008; Anav et al., 2013). In agroecosystems, the total leaf area of the crop canopy, is one of the key constraints on carbon assimilation and transpiration rates, which drive the accumulation of crop primary productivity (Gitelson et al., 2014). Therefore, LAI is required to estimate photosynthesis, evapotranspiration, crop yield, and many other physiological processes (Cao et al., 2015). EVI2 has frequently been used for crop growth and yield-related research as a remote sensing parameter (Kogan et al., 2012; Zhang et al., 2014; Huang et al., 2019; Liu et al., 2014). EVI-based crop growth metrics are much closer to capture crop status and growth characteristics, and growth metrics can be much more correlated to crop yield than an NDVI, (Huang et al., 2019). Similarly, this study used EVI indices to ensure that the crop yield estimation would be accurate.

LAI is one of the important parameters that reflects crop growth stages of vegetation and is widely used in quantitative analysis of crop models (Parker 2020; Yan et al. 2019). (Parker 2020), reiterates on the importance of leaf area index (LAI) by discussing remote sensing models used in its estimation. Several studies have extracted biophysical parameters from satellite imagery (Hui and Yao 2018; Yu et al. 2019) and assimilated them in simulation models. (Kang and Özdoğan 2019), successfully assimilated Landsat-derived LAI time series into crop model simulations using ensemble Kalman filter for individual fields or pixels. The covariance correlation matrix between the extracted and observed data for the LAI was R2 0.92549 for green gram as shown in Figure 3.0. The results used in the correlation matrix is shown in Table 2.

CONCLUSIONS

Relationships between LAI and VI vary depending on the crop, and the EVI or EVI2 derived from surface reflectance are the most accurate measures to use. The most important thing that this work has contributed is the confirmation that satellite LAI is capable of providing accurate data for monitoring crop growth in regions where resources for crop monitoring are scarce. The ease with which VI can be generated through the use of remotely sensed images and the application of straightforward statistical relationships contributes to the practical value of this research. This is especially true considering that essential variables that are required for process-based methods are infrequently present and difficult to measure. In addition, the findings of this research would be helpful in addressing significant concerns regarding the monitoring of food security in semi-arid regions.

REFERENCES

- Akilu Tesfaye, A., & Gessesse Awoke, B. 2021. Evaluation of the saturation property of vegetation indices derived from sentinel-2 in mixed crop-forest ecosystem. *Spatial Information Research*, 29(1), 109–121. <https://doi.org/10.1007/S41324-020-00339-5/FIGURES/11>
- Anav, A.; Murray-Tortarolo, G.; Friedlingstein, P.; Sitch, S.; Piao, S.; Zhu, Z. 2013. Evaluation of Land Surface Models in Reproducing Satellite Derived Leaf Area Index over the High-Latitude Northern Hemisphere. Part II: Earth System Models. *Remote Sens.*, 5, 3637–3661
- Asner, G.P.; Scurlock, J.M.O.; Hicke, J.A. Global synthesis of leaf area index observations: Implications for ecological and remote sensing studies. *Glob. Ecol. Biogeogr.* 2003, 12, 191–205.
- Baret, F.; Guyot, G. Potentials and limits of vegetation indices for LAI and APAR assessment. *Remote. Sens. Environ.* 1991, 35, 161–173. [CrossRef]
- Boken, V. K., & Chandra, S. (n.d.). ESTIMATING LEAF AREA INDEX FOR AN ARID REGION USING SPECTRAL DATA. In *African Crop Science Journal* (Vol. 20, Issue 4).
- BoresjoeBronge, L. 2004. Satellite remote sensing for estimating leaf area index, FPAR and primary production. A literature review. http://inis.iaea.org/Search/search.aspx?orig_q=RN:37010020
- Bréda, N. J. J. 2003. Ground- based measurements of leaf area index: a review of methods, instruments and current controversies. *Journal of Experimental Botany*, 54(392), 2403–2417. <https://doi.org/10.1093/JXB/ERG263>
- Broge, N.; Leblanc, E. Comparing prediction power and stability of broadband and hyperspectral vegetation indices for estimation of green leaf area index and canopy chlorophyll density. *Remote. Sens. Environ.* 2001, 76, 156–172. [CrossRef]
- Cao, X.; Zhou, Z.; Chen, X.; Shao, W.; Wang, Z. 2015. Improving leaf area index simulation of IBIS model and its effect on water carbon and energy—A case study in Changbai Mountain broadleaved forest of China. *Ecol. Model.* 2015, 303, 97–104
- CHEN, J. M., & BLACK, T. A. 1992. Defining leaf area index for non- flat leaves. *Plant Cell & Environment*, 15(4), 421. <https://doi.org/10.1111/j.1365-3040.1992.tb00992.x>
- Demarty, J., Chevallier, F., Friend, A. D., Viovy, N., Piao, S., & Ciais, P. 2007. Assimilation of global MODIS leaf area index retrievals within a terrestrial biosphere model. *Geophysical Research Letters*, 34(15), doi:10.1029/2007GL030014.
- Fassnacht, K.S.; Gower, S.T.; MacKenzie, M.D.; Nordheim, E.V.; Lillesand, T.M. 1997. Estimating the leaf area index of North Central Wisconsin forests using the landsat thematic mapper. *Remote. Sens. Environ.*, 61, 229–245.
- Fernandes, R.; Plummer, S.; Nightingale, J.; Baret, F.; Camacho, F.; Fang, H.; Garrigues, S.; Gobron, N.; Lang, M.; Lacaze, R.; et al. 2014. Global Leaf Area Index Product Validation Good Practices. Version 2.0. Best Practice for Satellite-Derived Land Product Validation; Schaepman-Strub, G., Román, M., Nickeson, J., Eds.; Land Product Validation Subgroup (WGCV/CEOS); p. 76. Available online: <http://lpvs.gsfc.nasa.gov/documents.html>

- Food and Agriculture Organization of the United Nations (FAO). 2008. Terrestrial Essential Climate Variables for Climate Change Assessment, Mitigation and Adaptation; FAO: Rome, Italy,
- Ghebremicael, S. T., Smith, C. W., & Ahmed, F. B. 2012. Estimating the leaf area index (LAI) of black wattle from Landsat ETM+ satellite imagery. [Http://Dx.Doi.Org/10.1080/20702620.2004.10431769](http://Dx.Doi.Org/10.1080/20702620.2004.10431769), 201(1), 3–12. <https://doi.org/10.1080/20702620.2004.10431769>
- Gitelson, A. A. 2004. Wide Dynamic Range Vegetation Index for Remote Quantification of Biophysical Characteristics of Vegetation. *Journal of Plant Physiology*, 161(2), 165–173. <https://doi.org/10.1078/0176-1617-01176>
- Gitelson, A.A.; Peng, Y.; Arkebauer, T.J.; Schepers, J. 2014. Relationships between gross primary production, green LAI, and canopy chlorophyll content in maize: Implications for remote sensing of primary production. *Remote Sens. Environ.*, 144, 65–72
- Haboudane, D., Miller, J. R., Pattey, E., Zarco-Tejada, P. J., & Strachan, I. B. 2004. Hyperspectral vegetation indices and novel algorithms for predicting green LAI of crop canopies: Modeling and validation in the context of precision agriculture. *Remote Sensing of Environment*, 90(3), 337–352. <https://doi.org/10.1016/J.RSE.2003.12.013>
- Huang, X., Liu, J., Zhu, W., Atzberger, C., Liu, Q., 2019. The optimal threshold and vegetation index time series for retrieving crop phenology based on a modified dynamic threshold method. *Remote. Sens.* 11 (23), 2725. <https://doi.org/10.3390/rs11232725>.
- Huete, A. R. 1988. A soil-adjusted vegetation index (SAVI). *Remote Sensing of Environment*, 25(3), 295–309. [https://doi.org/10.1016/0034-4257\(88\)90106-X](https://doi.org/10.1016/0034-4257(88)90106-X)
- Huete, A., Justice, C., & van Leeuwen, W. 1999. MODIS VEGETATION INDEX (MOD 13) ALGORITHM THEORETICAL BASIS DOCUMENT Version 3.
- Hui, Jiang, and Liu Yao. 2018. “A Method to Upscale the Leaf Area Index (LAI) Using GF-1 Data with the Assistance of MODIS Products in the Poyang Lake Watershed.” *Journal of the Indian Society of Remote Sensing* 46 (4): 551–60. <https://doi.org/10.1007/s12524-017-0731-5>.
- Jaetzold, R. & Schmidt, H. 1983. Farm Management Handbook of Kenya: National Conditions and Farm Management Information, Vol. II: Part A. Western Kenya. Nairobi: Ministry of Agriculture.
- Jonckheere, I., Fleck, S., Nackaerts, K., Muys, B., Coppin, P., Weiss, M., & Baret, F. 2004. Review of methods for in situ leaf area index determination Part I. Theories, sensors and hemispherical photography. *Agricultural and Forest Meteorology*, 121(1–2), 19–35. <https://doi.org/10.1016/J.AGRFORMET.2003.08.027>
- Jung, M.; Reichstein, M.; Ciais, P.; Seneviratne, S.I.; Sheffield, J.; Goulden, M.L.; Bonan, G.; Cescatti, A.; Chen, J.; De Jeu, R.; et al. 2010. Recent decline in the global land evapotranspiration trend due to limited moisture supply. *Nature*, 467, 951–954.
- Kang, Y., Özdoğan, M., Zipper, S. C., Román, M. O., Walker, J., Hong, S. Y., Marshall, M., Magliulo, V., Moreno, J., Alonso, L., Miyata, A., Kimball, B., & Loheide, S. P. 2016. How Universal Is the Relationship between Remotely Sensed Vegetation Indices and Crop Leaf Area Index? A Global Assessment. *Remote Sensing* 2016, Vol. 8, Page 597, 8(7), 597. <https://doi.org/10.3390/RS8070597>

- Kang, Yanghui, and Mutlu Özdoğan. 2019. "Field-Level Crop Yield Mapping with Landsat Using a Hierarchical Data Assimilation Approach." *Remote Sensing of Environment* 228: 144–63. <https://doi.org/10.1016/j.rse.2019.04.005>.
- Kaufman, Y. J., & Tanré, D. 1992. Atmospherically Resistant Vegetation Index (ARVI) for EOS-MODIS. *IEEE Transactions on Geoscience and Remote Sensing*, 30(2), 261–270. <https://doi.org/10.1109/36.134076>
- Kinane, S. M., Montes, C. R., Albaugh, T. J., & Mishra, D. R. 2021. A model to estimate leaf area index in loblolly pine plantations using landsat 5 and 7 images. *Remote Sensing*, 13(6). <https://doi.org/10.3390/RS13061140>
- Knipling, E. B. 1970. Physical and physiological basis for the reflectance of visible and near-infrared radiation from vegetation. *Remote Sensing of Environment*, 1(3), 155–159. [https://doi.org/10.1016/S0034-4257\(70\)80021-9](https://doi.org/10.1016/S0034-4257(70)80021-9)
- Kogan, F., Salazar, L., Roytman, L., 2012. Forecasting crop production using satellitebased vegetation health indices in Kansas, USA. *Int. J. Remote Sens.* 33, 2798–2814. <https://doi.org/10.1080/01431161.2011.621464>
- Launay, M.; Guerif, 2005. Assimilating remote sensing data into a crop model to improve predictive performance for spatial applications. *Agric. Ecosyst. Environ.*, 111, 321–339. [CrossRef]
- Laurent, V. C. E., Schaepman, M. E., Verhoef, W., Weyeremann, J., & Chávez, R. O. 2014. Bayesian object- based estimation of LAI and chlorophyll from a simulated Sentinel- 2 top- of- atmosphere radiance image. *Remote Sensing of Environment*, 140(0), 318–329. <https://doi.org/10.1016/j.rse.2013.09.005>
- Liu, Q., Liang, S., Xiao, Z., & Fang, H. 2014. Retrieval of leaf area index using temporal, spectral, and angular information from multiple satellite data. *Remote Sensing of Environment*, 145(0), 25–37. <https://doi.org/10.1016/j.rse.2014.01.021>
- Mourad, R., Jaafar, H., Anderson, M., & Gao, F. 2020. Assessment of Leaf Area Index Models Using Harmonized Landsat and Sentinel-2 Surface Reflectance Data over a Semi-Arid Irrigated Landscape. *Remote Sensing* 2020, Vol. 12, Page 3121, 12(19), 3121. <https://doi.org/10.3390/RS12193121>
- Mutanga, O., & Skidmore, A. K. 2010. Narrow band vegetation indices overcome the saturation problem in biomass estimation. <https://doi.org/10.1080/01431160310001654923>, 25(19), 3999–4014. <https://doi.org/10.1080/01431160310001654923>
- Parker, Geoffrey G. 2020. "Tamm Review: Leaf Area Index (LAI) Is Both a Determinant and a Consequence of Important Processes in Vegetation Canopies." *Forest Ecology and Management* 477 (June). <https://doi.org/10.1016/j.foreco.2020.118496>.
- Qi, J., Kerr, Y. H., Moran, M. S., Wertz, M., Huete, A. R., Sorooshian, S., & Bryant, R. 2000. Leaf area index estimates using remotely sensed data and BRDF models in a semiarid region. *Remote Sensing of Environment*, 73(1), 18–30. [https://doi.org/10.1016/S0034-4257\(99\)00113-3](https://doi.org/10.1016/S0034-4257(99)00113-3)
- Republic of Kenya 2002. Machakos District Development Plan 2002-2008: Effective Management for Sustainable Economic Growth and Poverty Reduction. Nairobi, Kenya: Government Printer
- Republic of Kenya 2010. Mainstreaming Sustainable Land Management in Agro-Pastoral Production Systems of Kenya. UNDP Project Document-UNDPPIMS NO.3245, GEF ID 3370.

- Reyes-González, A.; Kjaersgaard, J.; Trooien, T.; Sánchez, D.G.R.; Sánchez-Duarte, J.I.; Preciado-Rangel, P.; Fortis-Hernandez, M. 2019. Comparison of Leaf Area Index, Surface Temperature, and Actual Evapotranspiration Estimated using the METRIC Model and In Situ Measurements. *Sensors*, 19, 1857
- Roy, D. P., Zhang, H. K., Ju, J., Gomez-Dans, J. L., Lewis, P. E., Schaaf, C. B., Sun, Q., Li, J., Huang, H., & Kovalsky, V. 2016. A general method to normalize Landsat reflectance data to nadir BRDF adjusted reflectance. *Remote Sensing of Environment*, 176, 255–271. <https://doi.org/10.1016/J.RSE.2016.01.023>
- Shisanya, C.A., Recha, C. & Anyamba, A. 2011. Rainfall Variability and Its Impact on Normalized Difference Vegetation Index in ASALs of Kenya. *International Journal of Geosciences* 2:36-47.
- Thenkabail, P. S., Smith, R. B., & de Pauw, E. 2000. Hyperspectral Vegetation Indices and Their Relationships with Agricultural Crop Characteristics. *Remote Sensing of Environment*, 71(2), 158–182. [https://doi.org/10.1016/S0034-4257\(99\)00067-X](https://doi.org/10.1016/S0034-4257(99)00067-X)
- Van den Hurk, B.J.; Viterbo, P.; Los, S.O. 2003 Impact of leaf area index seasonality on the annual land surface evaporation in a global circulation model. *J. Geophys. Res. Space Phys.*, 108, 108.
- Watson, D.J. 1947 Comparative physiological studies on the growth of field crops: I. variation in net assimilation rate and leaf area between species and varieties, and within and between years. *Ann. Bot.*, 11, 41–76.
- Yan, Guangjian, Ronghai Hu, Jinghui Luo, Marie Weiss, Hailan Jiang, Xihan Mu, Donghui Xie, and Wuming Zhang. 2019. “Review of Indirect Optical Measurements of Leaf Area Index: Recent Advances, Challenges, and Perspectives.” *Agricultural and Forest Meteorology* 265 (March 2018): 390–411. <https://doi.org/10.1016/j.agrformet.2018.11.033>.
- Yu, Yuanhe, Jinliang Wang, Guangjie Liu, and Feng Cheng. 2019. “Forest Leaf Area Index Inversion Based on Landsat OLI Data in the Shangri-La City.” *Journal of the Indian Society of Remote Sensing* 47 (6): 967–76. <https://doi.org/10.1007/s12524-019-00950-6>.
- Zhang, H. K., Chen, J. M., Huang, B., Song, H. H., & Li, Y. R. 2014. Reconstructing seasonal variation of Landsat vegetation index related to leaf area index by fusing with MODIS data. *IEEE Journal of Selected Topics in Applied Earth Observations and Remote Sensing*, 7(3), 950–960. <https://doi.org/10.1109/jstars.2013.2284528>